Biotechnology and Bioprocess Engineering 23: 31-38 (2018)
DOI 10.1007/s12257-017-0366-y

pISSN 1226-8372
eISSN 1976-3816

RESEARCH PAPER

Preparation and Characterization of a pH-responsive Polymer that Interacts with Microbial Transglutaminase during Affinity Precipitation

Sipeng Li, Jialing Chen, Xuanjun Zhang, Zhaoyang Ding, and Xuejun Cao

Received: 13 September 2017 / Revised: 30 December 2017 / Accepted: 18 January 2018

Abstract Microbial transglutaminase (MTG) has been widely used in the food and pharmaceuticals industries. In this study, MTG was purified using affinity precipitation with an affinity polymer (P_{MMDN}-T), which was synthesized using a pH-responsive polymer (P_{MMDN}) coupled with L-thyroxin as an affinity ligand. Interactions between MTG and P_{MMDN}-T were investigated using turbidimetric titration, zeta potential measurements, and low-field nuclear magnetic resonance (LF-NMR). We found different behaviors, architectures, and phase states of pH-dependent interactions between MTG and P_{MMDN}-T interactions. Binding energetics between MTG and P_{MMDN}-T were determined by isothermal titration calorimetry (ITC). The isoelectric point (p*I*) of the affinity polymer was 4.65 and was recovered with 96.7% efficiency after recycling the polymer three times. The optimal adsorption condition was 0.02 mol/L phosphate buffer (pH 6.0) with 1.0 mol/L NaCl at 30.0°C and a ligand density of 50.0 μmol/g. The maximum elution recoveries of total MTG were 98.44% (protein) with 92.19% (activity) using 0.02 mol/L pH 10.0 Gly-NaOH as the eluent.

Keywords: microbial transglutaminase, pH-responsive polymer, affinity precipitation, low-field nuclear magnetic resonance, isothermal titration calorimetry

Sipeng Li, Jialing Chen, Zhaoyang Ding*, Xuejun Cao*
State Key Laboratory of Bioreactor Engineering, Department of Bioengineering, East China University of Science and Technology, Shanghai 200-237, China
Tel: +86-21-642-52695; Fax: +86-21-642-52695
E-mail: caoxj@ecust.edu.cn
E-mail: zhaoyangding@umac.mo

Xuanjun Zhang, Zhaoyang Ding
Faculty of Health Sciences, University of Macau, Macau SAR, China

1. Introduction

Affinity chromatography for protein separation and purification from crude aqueous solutions has limitations [1-4]. These limitations include problems in scaling-up the purification due to increasing column pressure and low adsorption capacity due to steric hindrance and slow binding due to mass transfer [5,6]. Affinity precipitation could overcome these problems in several ways. Selective ligands are immobilized on the recycled polymer, and the affinity polymer and is applied to adsorb the target protein from the aqueous solution followed by precipitation, desorption and recovery. Therefore, target proteins are purified in a single step and are easily scaled up with an option to continuously purify protein [7-10].

Among the affinity precipitation polymers, we focused on a pH-responsive polymer with L-thyroxin as the affinity ligand. The pH-responsive affinity polymer precipitate changes with pH and is quickly separated in water. It is thought that electrostatic interactions between negatively charged carboxyl groups on the polymers and the positively charged proteins are pH-responsive and form these complexes used in purification [11-15]. L-Thyroxin is a derivative of tyrosine and is a hormone secreted by follicular cells. It can interact with many kinds of proteins in the blood serum and can be a potential and safe affinity ligand. We previously studied the affinity polymer P_{MMDN}-T to separate lysozyme [16] as well as its affinity interactions with MTG [17, 18]. MTG (EC 2.3.2.13) catalyzes the formation of a crosslink between a free amine group from a bound protein and a γ-carboxyamide group from the glutamine of a bound peptide [19]. Due to these properties, MTG is widely used in food and pharmacy applications [20-22]. Knowing these

important MTG applications, we used MTG as the target enzyme to study the affinity precipitation process.

In light of our previous reports on affinity precipitation, we sought to characterize P_{MMDN}-T for selective precipitation of proteins in this study and gain a better understanding of their precipitation behavior. Interactions between MTG and P_{MMDN}-T were investigated using a combination of turbidimetric titration, zeta potential measurement, and low-field nuclear magnetic resonance. These methods revealed different behaviors and phase states of pH-dependent interactions between MTG and P_{MMDN}-T. Additionally, the binding energetics between MTG and P_{MMDN}-T were determined by isothermal titration calorimetry (ITC). We found that the adsorption levels of MTG on P_{MMDN}-T are regulated by pH and ionic strength. Understanding the mechanism between MTG and P_{MMDN}-T interactions allows for the purification or separation of MTG by P_{MMDN}-T under optimal conditions.

For affinity precipitation of MTG, a pH-responsive polymer with L-thyroxin as the affinity ligand was developed. The prepared affinity polymer, P_{MMDN}-T, could be precipitated from the solution at pH 4.65 (p*I*), and the recovery was 96.7%. The adsorption and desorption conditions were optimized for MTG recovery. The results of electrophoresis showed the suitability of affinity precipitation methods in the purification of MTG from the fermentation broth. The study of the interactions between MTG and P_{MMDN}-T provides substantial information about the affinity precipitation of MTG and helps establish a specific strategy for MTG purification.

2. Materials and Methods

2.1. Materials

Methyl acrylic acid (MAA), methyl methacrylate (MMA), methacrylic acid 2-(dimethylamino) ethylester (DMAEMA), N-methylolacrylamide(N-MAM), and azobisisobutyronitrile (AIBN) were purchased from the Sinopharm Chemical Reagent Co., Ltd. (Shanghai, China). L-thyroxin, pure MTG, L-glutaminehydroxylamine, and N-carboxybenzoyl-L-glutaminyl-glycine (N-CBZ-Gln-Gly) were purchased from Sigma (St. Louis, USA). All chemicals were of analytical grade.

The fermentation broth in this study was provided by Jiangsu Yiming Biological Co., Ltd. The production of MTG was carried out using a mutant of *Streptoverticillium mobaraense*. Starch, glucose, peptone, yeast extract, $MgSO_4$, K_2HPO_4 and KH_2PO_4 at different concentrations were used in the fermentation medium. After cultivation, the cells and other precipitates were removed. All these samples were kept at -20°C.

2.2. Preparation of affinity polymers

Ding's method was followed for polymer synthesis [23]. Four monomers (MAA, MMA, DMAEMA and N-MAM) were combined in a flask in a nitrogen atmosphere for 15 min using AIBN as the polymerization initiator and absolute ethanol as the solvent. The N-MAM monomer presents a hydroxyl group for the ligand to connect to the polymer during the activation step. The activation reaction was carried out for 24 h at 60.0°C. Next, the product was precipitated and washed three times in acetone and absolute ethanol. Subsequently, the precipitate was vacuum dried. Epichlorohydrin (ECH) was introduced to connect the L-thyroxin to the polymer (P_{MMDN}). P_{MMDN} (1.0%, w/v) was dissolved in 1.0 mol/L NaOH with varying amounts of ECH in a constant-temperature bath at 60.0°C for 24 h. Different amounts of L-thyroxin were added to the polymer-ECH at 40.0°C for 2 h, and the P_{MMDN}-T was precipitated by adding HCl (1.0 mol/L). P_{MMDN}-T was purified by filtration and vacuum drying. The supernatant was collected, and the ligand density of the P_{MMDN}-T was determined using mass balance calculations.

2.3. Adsorption and desorption experiments

2.3.1. Adsorption of MTG

P_{MMDN}-T was dissolved in aqueous solution to a concentration of 2.0% (w/v). Next, 2.5 mL of P_{MMDN}-T solution was mixed with 2.5 mL of MTG solution of varied concentrations. The adsorption experiments were carried out for 2 h at 25.0°C within a water bath shaker at 100 rpm. After the reaction, the pH of the solution was adjusted by HCl (0.1 mol/L) to the p*I* of polymer, which was then collected. The adsorption to amount of P_{MMDN}-T was investigated by varying the time, pH (3.0 ~ 10.0 buffers), ionic strength (0.0 ~ 1.0 mol/L NaCl), ligand density (10.0 ~ 90.0 μmol/g), temperature (10.0 ~ 60.0°C), and adsorption isotherm. All tests were repeated in triplicate.

2.3.2. Desorption of MTG

The collected precipitate was dissolved in 5.0 mL of various eluents. Desorption stages were carried out within 2 h of shaking at 100 rpm at 25.0°C in a water bath. P_{MMDN}-T was collected by the same method as the adsorption step for use in the next cycle. When appropriate, the desorption step was repeated with different eluents. After obtaining MTG, its activity [24] and protein concentration were measured.

Two solutions were prepared for enzyme activity measurements. Solution S: 0.347 g hydroxylamine hydrochloride, 0.154 g reduced glutathione, and 0.506 g N-CBZ-Gln-Gly were dissolved in 50.0 mL 0.2 mol/L Tris–HCl buffer, and the final pH of this solution was adjusted to 6.0.

Solution T: equal volumes of 5% $FeCl_3$ solution, 3 mol/L HCl, and 12% trichloroacetic acid were mixed. Pure MTG solution (0.2 mL) at different concentrations was added to Solution S (0.8 mL). The mixture was kept in a water bath (37°C) for 10 min. Next, 1.0 mL of Solution T was added to end the reaction. The final solution was centrifuged for 5 min at 5,000 rpm, and the absorbance of the supernatant at 525 nm was determined. One unit of MTG activity could be defined as the amount of MTG that catalyzed the formation of 1 μmol/L L-Glutamic acid γ-monohydroxamate (L-Glu(γ)HXM) per minute at 37°C. Different concentrations of L-Glu(γ)HXM were prepared for the enzyme activity measurements to make a standard curve.

2.3.3. Affinity precipitation of MTG from fermentation broth

MTG was separated from the fermentation broth by P_{MMDN}-T using optimal adsorption and desorption conditions. The fermentation broth was centrifuged at 4,000 rpm for 10 min to remove visible precipitation. After affinity precipitation, the protein component in the broth and in the desorbed solution was determined using sodium dodecyl sulfate polyacrylamide gel electrophoresis (SDS-PAGE).

2.4. Isothermal titration calorimetry

Isothermal titration calorimetry (ITC) experiments were performed with a Microcal ITC200 (GE Healthcare, USA). The thermodynamic quantities of MTG binding onto P_{MMDN}-T were determined by ITC. All sample solutions were made in 5.0 mM MES buffer at various pH values and filtered using 0.22 μm filters. Injections (4.0 μL) of P_{MMDN}-T solution (500.0 μM) were made from an auto-controlled microsyringe at 3.0 min intervals into the sample solution containing MTG (25.0 μM) while stirring at 1,000 rpm at 25.0°C. Control experiments were performed with identical injections into the cell, containing buffer without MTG, and showed insignificant heats of dilution. The experimental data were fitted to a theoretical titration curve using Microcal Origin software with ΔH (enthalpy change in kJ/mol) and K_a (adsorption constant in /M) [25]. Thermodynamic-binding parameters were calculated from the equation:

$$\Delta G = \Delta H - T\Delta S = -RTlnK_a \quad (1)$$

where ΔG, ΔH, and ΔS are the changes in free energy, enthalpy, and entropy of binding [26-28]. T is the absolute temperature and R = 1.98 cal/mol/K.

2.5. Zeta potential measurement

The zeta potentials of polymers, MTG and polymer-MTG complexes were determined by a Zetasizer Nano ZEN3600 (Malvern, UK) at variable pH values at 25.0°C. The pH of the sample solutions (10.0 ppm) was adjusted with HCl and NaOH. Determination of the zeta potential was used to determine the isoelectric point (pI) of the polymer [29,30].

2.6. Turbidimetric titration

Transmittance (%T) was monitored with a colorimeter (Brinkmann PC 950, Germany) using a 420 nm filter to calculate the turbidity at 100%T with transmittance fluctuations (± 0.1%). All samples were prepared with DI water and filtered using 0.45 μm filters. A Ross Ultra Combination pH meter (Orion, USA) was used to monitor the pH of the sample solutions. The turbidity of the samples from pH 10.0 to 2.0 was obtained by the addition of 0.1 M HCl. The polymer and MTG concentrations were 0.020 and 0.008 mg/mL, respectively. A nitrogen purge was performed during all titrations. Blank samples of polymer and MTG were subtracted to eliminate their effects in isolation [31,32].

2.7. Low-field nuclear magnetic resonance

To investigate the effects of pH on the interactions between polymers and MTG, their properties were measured using transverse relaxation time (T) on a Niumag Benchtop Pulsed NMR analyzer PQ001 (Niumag Electric, China). The magnetic field strength was set at 0.5 ± 0.08 T, and the corresponding resonance frequency for protons was 21.3 MHz [33]. Samples of P_{MMDN} (2.0%, w/v), P_{MMDN}-T (2.0%, w/v) and MTG (0.4%, w/v) were prepared in various buffers of different pH values from 3.5 to 6.0 for use as standards.

3. Results and Discussion

The affinity polymer P_{MMDN}-T has been reported previously [16]. It has successfully been applied to separate lysozyme from salted duck white. The properties of MTG are different from lysozyme, and therefore, the conditions of affinity precipitation for MTG also needed to be optimized in this study.

3.1. Adsorption of MTG

Incubation time, ionic strength, pH, ligand densities, temperature and adsorption isotherms were investigated to understand the factors affecting MTG adsorption. The adsorption kinetic curve of MTG binding to P_{MMDN}-T is shown in Fig. 1A. Fast adsorption behavior was observed during the first hour of the adsorption process, and then the adsorption equilibrium was achieved gradually over approximately 2.0 h. The adsorption time to attain equilibrium MTG binding to P_{MMDN}-T was influenced by the concentration of free MTG in the solution and the adsorption capacity of P_{MMDN}-T.

The effect of ionic strength on the adsorption of MTG is

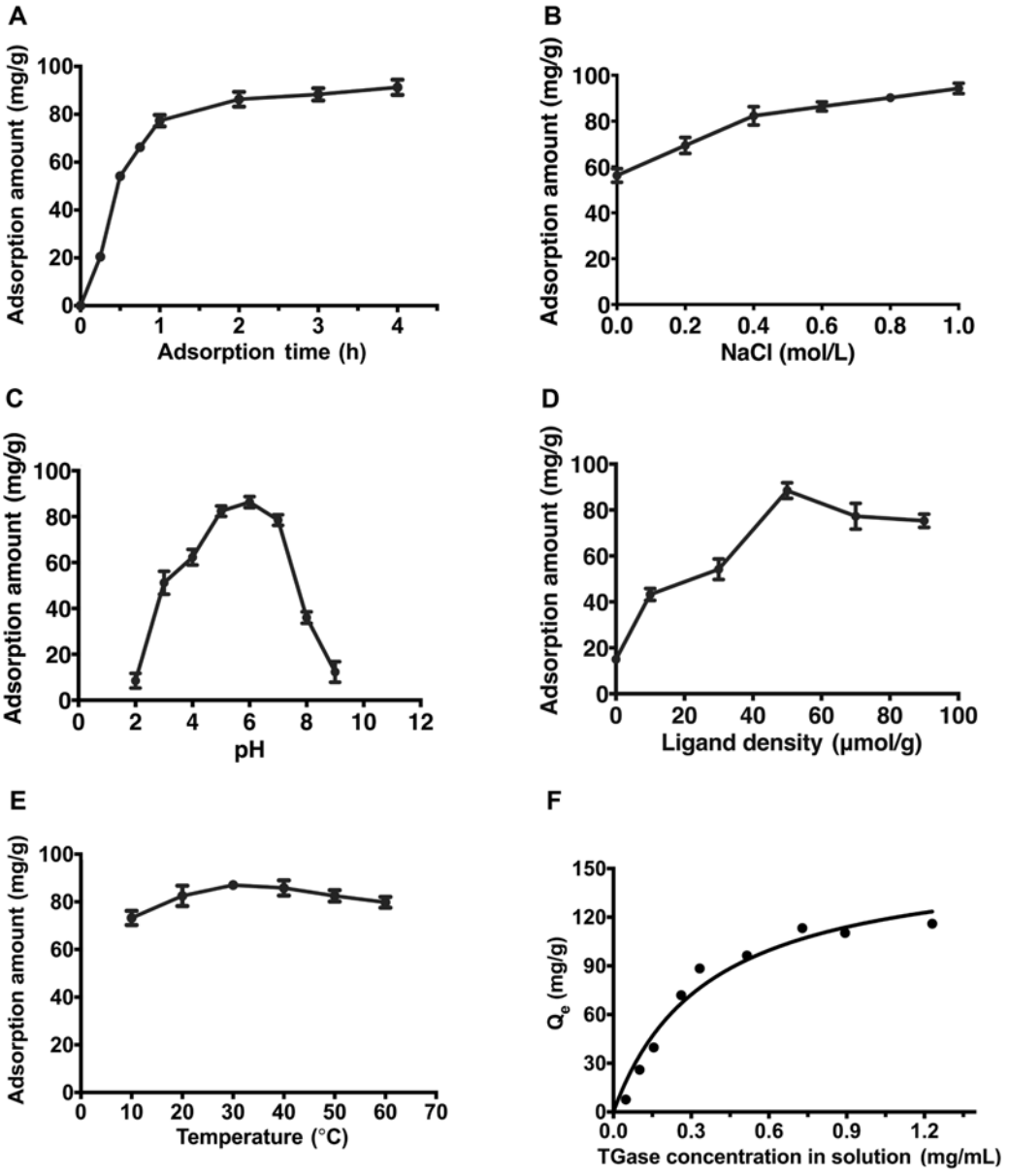

Fig. 1. Study of adsorption conditions of MTG on P_{MMDN}-T. (A) The effect of reaction time for MTG adsorption onto the P_{MMDN}-T. Initial concentration of MTG 4.0 mg/mL, temperature = 30.0°C, pH = 6.0, and affinity ligand density 50.0 μmol/g. (B) The effect of ionic strength for MTG adsorption onto the P_{MMDN}-T. Initial concentration of MTG 4.0 mg/mL, temperature = 30.0°C, pH = 6.0, affinity ligand density 50.0 μmol/g. (C) The effect of pH for MTG adsorption onto the P_{MMDN}-T. Initial concentration of MTG 4.0 mg/mL, temperature = 30.0°C, NaCl concentration 1.0 mol/L, and affinity ligand density 50.0 μmol/g. (D) The effect of ligand density for MTG adsorption onto the P_{MMDN}-T. Initial concentration of MTG 4.0 mg/mL, temperature = 30.0°C, pH = 6.0, and NaCl concentration 1.0 mol/L. (E) The effect of temperature for MTG adsorption onto the P_{MMDN}-T. Initial concentration of MTG 4.0 mg/mL, NaCl concentration 1.0 mol/L, pH = 6.0, and ligand density 50.0 μmol/g. (F) Adsorption isotherm for MTG binding onto the affinity polymer. Temperature = 30.0°C, pH = 6.0, NaCl concentration 1.0 mol/L, and affinity ligand density 50.0 μmol/g.

presented in Fig. 1B. As the NaCl concentration is increased, the adsorbed amount of MTG also increased. Additional salts removed surface charges of P_{MMDN}-T and MTG, which allowed weaker electrostatic repulsive interactions between them. Furthermore, hydrophobic interactions involving MTG were also affected by adding salts.

The effect of pH on adsorption of MTG was presented in Fig. 1C. The highest adsorption amount (88.7 mg MTG/g P_{MMDN}-T) was achieved near pH 6.0, with decreased adsorption amounts at lower and higher pH values. The surface charges were zero when the pH of the solutions achieved the p*I* of P_{MMDN}-T and MTG at 4.6 and 9.0, respectively. Around these p*I* values, the adsorption amount should be lower because of lower electrostatic interactions

between them. At pH values between 4.6 and 9.0, the surface charge of the P_{MMDN}-T was negative and MTG was positive, which resulted in high adsorption values.

The effect of ligand density on adsorption of MTG is presented in Fig. 1D. Maximum adsorption was observed with ligand densities of approximately 50.0 μmol/g. Adsorption amounts increased as ligand densities decreased below 50.0 μmol/g. At higher ligand densities, the adsorption amount stabilized and then decreased slightly. Additional ligands on the polymer likely increased steric hindrance, which, therefore, decreased binding potential between the ligand and MTG. A ligand density of 50.0 μmol/g for P_{MMDN}-T was chosen for subsequent experiments.

Fig. 1E shows the effect of temperature on adsorption of MTG, and Fig. 1F displays MTG adsorption isotherms at different temperatures. Maximal adsorption occurred near 30.0°C. From 10.0 to 30.0°C, proteins exposed hydrophobic amino acids, which could increase the binding area and affinity between MTG and P_{MMDN}-T. However, monomeric DM in P_{MMDN}-T was thermoresponsive, resulting in tiny polymer aggregates that decreased the adsorbed amounts.

Langmuir equation (2) was chosen to describe the adsorption isotherm of MTG:

$$q = \frac{Q_m C}{K_d + C} \tag{2}$$

where C (mg/mL) is the concentration of free MTG in the solution and q (mg/g) is the MTG adsorption capacity. Q_m (mg/g) is the maximum adsorbed amount, and K_d (mg/mL) is the dissociation constant. The calculated determination coefficient (R^2) of the Langmuir model was 0.96, which indicated that the model fits well. Q_m and K_d calculated from the equation were 160.01 mg/g and 0.36 mg/mL, respectively. From the molecular weight of MTG, this Q_m value is equivalent to 4.21 μmol/g of affinity polymer and K_d is equivalent to 9.47 μmol/L.

3.2. Desorption of MTG

The interactions between MTG and affinity polymer were affected by temperature, ionic strength, ligand density and pH values. Additionally, some surfactants also were applied in the desorption step of affinity purification. Desorption of bound MTG under various conditions (different kinds of salts or surfactants, salt concentration, pH) is shown in Table 1. The optimized desorption condition was 0.02 mol/L Gly-NaOH buffer (pH 10.0). Under these conditions, 98.44% (protein amount) and 92.19% (enzyme activity) of the adsorbed MTG were desorbed from P_{MMDN}-T. In contrast to adsorption optimizations, low ionic strength should reduce interactions between MTG and L-thyroxin and yield higher elution recovery. As shown in Table 1, elution recoveries of MTG were not good using high salt concentrations, which were consistent with the observation that additional NaCl enhanced adsorption of MTG onto P_{MMDN}-T.

Table 1. Desorption conditions and results

No.	Eluants	MTG amount (%)	MTG activity (%)
1	0.5 mol/L NaSCN	44.69	54.21
2	1.0 mol/L NaSCN	31.51	29.09
3	0.1 mol/L EDTA	50.34	54.76
4	1.0 mol/L KSCN	39.21	42.14
5	pH 7.0 PB + 0.5 mol/L Urea	25.35	30.91
6	pH 7.0 PB + 1.0% Triton 100	95.50	78.13
7	pH 7.0 PB + 20% Glycol	86.28	40.19
8	pH 8.0 PB	38.20	39.44
9	pH 9.0 Gly-NaOH	58.01	54.30
10	pH 10.0 Gly-NaOH	98.44	92.19

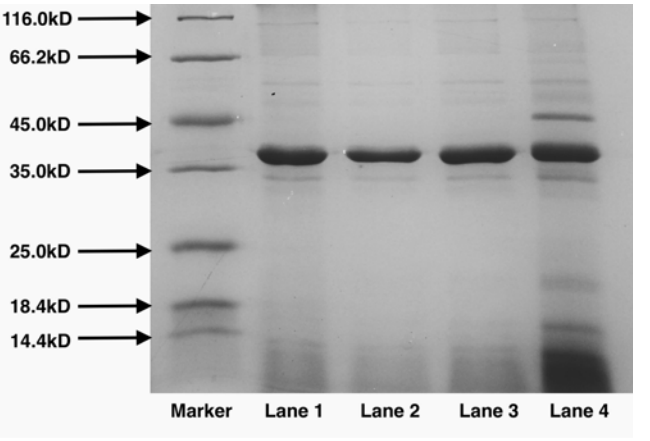

Fig. 2. Separation of MTG from fermentation broth. Marker; Lane 1, MTG desorbed by pH 7.0 PB + 1.0% Triton 100; Lane 2, MTG desorbed by pH 10.0 Gly-NaOH; Lane 3, pure MTG; Lane 4, MTG fermentation broth.

Next, the separation of MTG from MTG fermentation broth was investigated next. Previously obtained optimal adsorption and desorption conditions were applied to these experiments and analysis carried out using SDS-PAGE [34]. The gels used in the experiments were 15.0% acrylamide gel, and the final gels were stained with 0.25% Coomassie Brilliant Blue R-250. According to SDS-PAGE, the MTG molecular weight was 38.0 kDa. Lanes 1 ~ 3 show a single band; however, lane 1 was impure according to the graph because the protein was denatured by Triton. Pure MTG is seen in the gel when pH 10.0 Gly-NaOH buffer was used as eluent (lane 2).

3.3. Isothermal titration calorimetry

ITC was used to investigate the energetics of the interactions

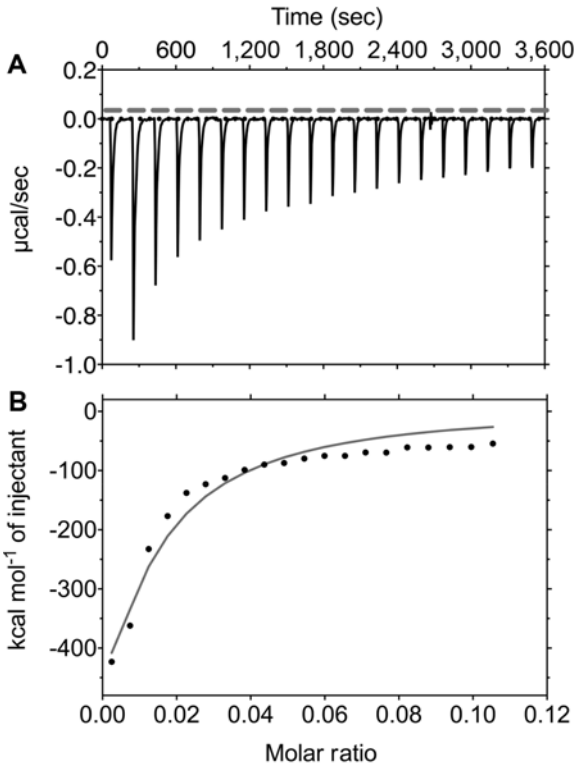

Fig. 3. Isothermal titration calorimetry results for MTG adsorbed onto P_{MMDN}-T at pH 7.0 in 5 mM MES buffer. (A) Raw data from the ITC experiment. (B) Integrated heat of each injection (dot) and one-site adsorption fitting (solid line).

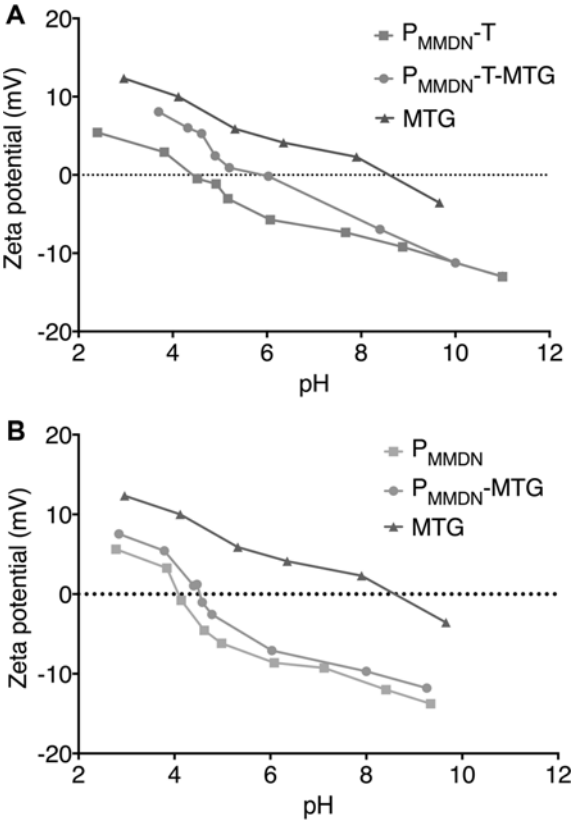

Fig. 4. Zeta potentials of MTG, P_{MMDN}, P_{MMDN}-T and the complexes at different pH values. (A) The comparison for MTG, P_{MMDN}-T and their complexes. (B) The results for MTG, P_{MMDN} and their complexes.

between MTG and P_{MMDN}-T. Fig. 3A presents the ITC raw data for MTG binding to P_{MMDN}-T. Each negative peak corresponded to the heat released by the injection of MTG, which indicated that the binding of MTG to P_{MMDN}-T was exothermic. The exothermic nature of the reaction further supports the idea that affinity binding in this instance is primarily driven by electrostatic interactions. Integration of the area under the negative exothermic peaks provided a binding isotherm (Fig. 3B) of MTG adsorption to P_{MMDN}-T, which had multiple identical binding sites independently available for MTG binding.

MTG adsorption to charged polymers usually leads to an increase in entropy because either the counterion or water is released. These two situations should be considered for entropy changes in a system. External energy would be needed to release water molecules inside the P_{MMDN}-T structure during adsorption. However, the MTG adsorbing onto P_{MMDN}-T reduces entropy by releasing the counterion from MTG molecules. These two situations should be considered for the entropy change of the system. The entropy change was also determined to be negative using ITC because the entropic reduction associated with MTG adsorption is larger than the entropic gain associated with MTG adsorption. Therefore, MTG adsorption to the P_{MMDN}-T was the major effect.

3.4. Zeta potential measurements

Fig. 4 shows zeta potentials for the solutions of MTG, P_{MMDN}, P_{MMDN}-T and their complexes. The zeta potentials of all of the samples decreased as pH increased. The p*I* was determined as the pH where the zeta potential is zero. The p*I* of P_{MMDN} was 4.51 and of P_{MMDN}-T was 4.69 [16, 35]. As shown in Fig. 4A, the MTG showed a higher zeta potential than P_{MMDN}-T at all pH ranges tested. With the adsorption of MTG, the zeta potential of P_{MMDN}-T increased between the pH ranges from 4.0 to 9.0, which could be correlated with the previous adsorption experiments. Around pH 6.0, the zeta potential of the complexes was close to zero because of formation of high adsorption amounts. The interactions of P_{MMDN} and MTG showed a similar trend.

3.5. Turbidimetric titration

In this affinity precipitation system, adsorption and desorption were reversible. The pH range for the adsorption interactions

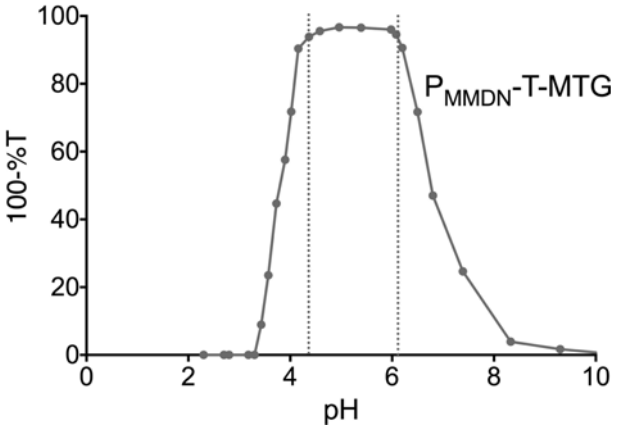

Fig. 5. Turbidimetric titration for the mixture of P_{MMDN}-T and MTG at various pH values.

between P_{MMDN}-T and MTG was determined by turbidimetric titrations by adding HCl to mixtures of high pH as shown in Fig. 5. The results show that the adsorption of MTG to P_{MMDN}-T occurred from pH 4.5 to 6.2, which confirmed the adsorption experiment data. When the pH was within this range, the charges of P_{MMDN}-T and MTG were opposite, leading to a strong attractive interaction.

3.6. Low-field NMR relaxation measurements

The LF-NMR T_2 relaxation time reflects water mobility inside the polymer or the complexes formed. According to the curves in Fig. 6, water molecules in P_{MMDN}-T were more fluid. However, water molecules in the P_{MMDN}-T and MTG complex decreased from pH 4.6 to 5.8 and increased from pH 5.8 onwards. The lowest T_2 relaxation time occurred at pH 5.8, and this indicates that water molecules inside the complex were more stable than the other pH values tested. This result corresponded to the adsorption experiment and could be due to the change of electrical charge distribution and quantity on the P_{MMDN}-T and MTG complexes at various pH values.

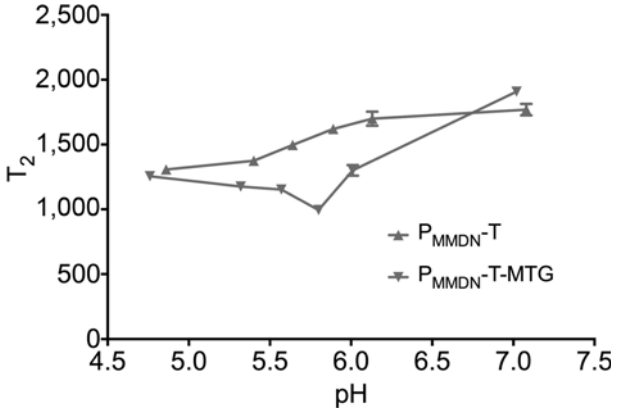

Fig. 6. T_2 relaxation time of P_{MMDN}-T with MTG at different pH value.

4. Conclusion

The pH-responsive polymer immobilized L-thyroxin was used as an affinity ligand for the affinity precipitation of MTG in water. The optimal adsorption and desorption conditions were determined experimentally. The turbidimetric titration and zeta potential measurements explained how the highest amounts were absorbed. The ITC results indicated an exothermic energy change, and LF-NMR showed water inside the complex of P_{MMDN}-T and MTG during the precipitation process. Electrophoretically pure MTG was also collected using P_{MMDN}-T from a culture according to our conditions. A specific strategy for the separation of MTG was established by a pH-responsive affinity polymer P_{MMDN}-T. Analysis of the interactions offers a clear roadmap for affinity ligand screening, purification conditions optimization, affinity polymer preparation and other aspects. The results of this study help understand how protein separation works using a pH-responsive polymer, which can be used in a wide variety of applications.

Acknowledgement

This research was partially supported by the FDCT grant 052/2015/A2 from the Macau government.

References

1. Cuatrecasas, P. and C. B. Anfinsen (1971) Affinity chromatography. *Annu. Rev. Biochem* 40: 259-278.
2. Vunnum, S., S. R. Gallant, Y. J. Kim, and S. M. Cramer (1995) Immobilized metal affinity chromatography: Modeling of nonlinear multicomponent equilibrium. *Chem. Eng. Sci*. 50: 1785-1803.
3. Subramanian, S. and P. D. Ross (1984) Dye-ligand affinity chromatography: The interaction of Cibacron Blue F3GA® with proteins and enzyme. *Crit. Rev. Biochem. Mol. Biol*. 16: 169-205.
4. Porath, J., J. A. N. Carlsson, I. Olsson, and G. Belfrage (1975) Metal chelate affinity chromatography, a new approach to protein fractionation. *Nature* 258: 598-599.
5. Freitag, R., I. Schumacher, and F. Hilbrig (2007) Affinity precipitation an option for early capture in bioprocessing. *Biotechnol. J*. 2: 685-690.
6. Teotia, S., R. Lata, S. K. Khare, and M. N. Gupta (2001) One-step purification of glucoamylase by affinity precipitation with alginate. *J. Mol. Recognit*. 14: 295-299.
7. Gupta, M. N., R. Kaul, D. Guoqiang, U. Dissing, B. Mattiasson, and W. H. Scouten (1996) Affinity precipitation of proteins. *J. Mol. Recognit.* 9: 356-359.
8. Mattiasson, B., A. Kumar, and I. Y. Galaev (1998) Affinity precipitation of proteins: Design criteria for an efficient polymer.

J. Mol. Recognit. 11: 211-216.
9. Eggert, M., T. Baltes, F. Garret-Flaudy, and R. Freitag (1998) Affinity precipitation – an alternative to fluidized bed adsorption. *J. Chromatogr. A* 827: 269-280.
10. Arnold, L. and R. Chen (2014) Novel thermo-responsive fucose binding ligands for glycoprotein purification by affinity precipitation. *Biotechnol. Bioeng.* 111: 413-417.
11. Chern, C. S., C. K. Lee, C. Y. Chen, and M. J. Yeh (1996) Characterization of pH-sensitive polymeric supports for selective precipitation of proteins. *Colloids Surf. B: Biointer.* 6: 37-49.
12. Bulmus, V., Z. Ding, C. J. Long, P. S. Stayton, and A. S. Hoffman (2000) Site-specific polymer-streptavidin bioconjugate for pH-controlled binding and triggered release of biotin. *Bioconjug. Chem.* 11: 78-83.
13. Hoffman, A. S. and P. S. Stayton (2007) Conjugates of stimuli-responsive polymers and proteins. *Prog. Polym. Sci.* 32: 922-932.
14. Mattiasson, B., A. Kumar, A. E. Ivanov, and I. Y. Galaev (2007) Metal-chelate affinity precipitation of proteins using responsive polymers. *Nat. Protoc.* 2: 213-220.
15. Ding, Z., L. Kang, J. Liu, X. Zhang, and X. Cao (2017) Preparation of pH-responsive metal chelate affinity polymer for adsorption and desorption of insulin. *J. Chem. Technol. Biotechnol.* 92: 1590-1595.
16. Ding, Z., S. Li, and X. Cao (2014) Separation of lysozyme from salted duck egg white by affinity precipitation using pH-responsive polymer with an l-thyroxin ligand. *Sep. Purif. Technol.* 138: 153-160.
17. Ding, Z., S. Li, and X. Cao (2015) Microbial transglutaminase separation by pH-responsive affinity precipitation with Crocein Orange G as the ligand. *Appl. Biochem. Biotechnol.* 177: 253-266.
18. Li, S., Z. Ding, and X. Cao (2016) Separation of transglutaminase by thermo-responsive affinity precipitation using l-thyroxin as ligand. *SpringerPlus*. 5: 37.
19. Ando, H., M. Adachi, K. Umeda, A. Matsuura, M. Nonaka, R. Uchio, H. Tanaka, and M. Motoki (1989) Purification and characteristics of a novel transglutaminase derived from microorganisms. *Agric. Biol. Chem.* 53: 2613-2617.
20. Gaspar, A. L. C. and S. P. de Góes-Favoni (2015) Action of microbial transglutaminase (MTGase) in the modification of food proteins: A review. *Food Chem.* 171: 315-322.
21. Oteng-Pabi, S. K., C. Pardin, M. Stoica, and J. W. Keillor (2014) Site-specific protein labelling and immobilization mediated by microbial transglutaminase. *Chem. Commun.* 50: 6604-6606.
22. Chen, P. -Y., K. -C. Yang, C. -C. Wu, J. -H. Yu, F. -H. Lin, and J. -S. Sun (2014) Fabrication of large perfusable macroporous cell-laden hydrogel scaffolds using microbial transglutaminase. *Acta Biomater.* 10: 912-920.
23. Ding, Z. and X. Cao (2013) Affinity precipitation of cellulase using pH-response polymer with Cibacron Blue F3GA. *Sep. Purif. Technol.* 102: 136-141.
24. Grossowicz, N., E. Wainfan, E. Borek, and H. Waelsch (1950) The enzymatic formation of hydroxamic acids from glutamine and asparagine. *J. Biol. Chem.* 187: 111-125.
25. Kayitmazer, A. B., D. Seeman, B. B. Minsky, P. L. Dubin, and Y. Xu (2013) Protein–polyelectrolyte interactions. *Soft Matt*. 9: 2553-2583.
26. Freyer, M. W. and E. A. Lewis (2008) Isothermal titration calorimetry: experimental design, data analysis, and probing macromolecule/ligand binding and kinetic interactions. *Method Cell Biol.* 84: 79-113.
27. Velazquez-Campoy, A. and E. Freire (2006) Isothermal titration calorimetry to determine association constants for high-affinity ligands. *Nat. Protoc.* 1: 186-191.
28. Freire, E. (2004) Isothermal titration calorimetry. *Curr. Protoc. Cell Biol*. 17: 1-17.18.
29. Wang, S., K. Chen, Y. Xu, X. Yu, W. Wang, L. Li, and X. Guo (2013) Protein immobilization and separation using anionic/cationic spherical polyelectrolyte brushes based on charge anisotropy. *Soft Matt*. 9: 11276.
30. Karg, M., I. Pastoriza-Santos, B. Rodriguez-González, R. Von Klitzing, S. Wellert, and T. Hellweg (2008) Temperature, pH, and ionic strength induced changes of the swelling behavior of PNIPAM-poly(allylacetic acid) copolymer microgels. *Langmuir*. 24: 6300-6306.
31. Wang, H., Y. Wang, L. Yuan, L. Wang, W. Yang, Z. Wu, D. Li, and H. Chen (2013) Thermally responsive silicon nanowire arrays for native/denatured-protein separation. *Nanotechnol*. 24: 105101.
32. Wang, S., K. Chen, A. B. Kayitmazer, L. Li, and X. Guo (2013) Tunable adsorption of bovine serum albumin by annealed cationic spherical polyelectrolyte brushes. *Colloids Surf. B: Biointer.* 107: 251-256.
33. Hou, H. and X. Cao (2015) pH recycling aqueous two-phase systems applied in extraction of Maitake β-Glucan and mechanism analysis using low-field nuclear magnetic resonance. *J. Chromatogr. A* 1405: 40-48.
34. Laemmli, U. K. (1970) Cleavage of structural proteins during the assembly of the head of bacteriophage T4. *Nature* 227: 680-685.
35. Yan, B. and X. Cao (2012) Preparation of aqueous two-phase systems composed of two pH-response polymers and liquid–liquid extraction of demeclocycline. *J. Chromatogr. A* 1245: 39-45.